Respiratory Research

RESEARCH

Open Access

Computed tomography morphological assessments of central airways in interstitial lung abnormalities and idiopathic pulmonary fibrosis

Tomoki Maetani[1], Naoya Tanabe[1*], Kiminobu Tanizawa[1], Ryo Sakamoto[2], Yusuke Shiraishi[1], Yusuke Hayashi[1], Michihiro Uyama[1], Atsushi Matsunashi[1], Susumu Sato[1,3], Katsuhiro Suzuki[4], Izuru Masuda[5], Motonari Fukui[6], Shizuo Kaji[7], Tomohiro Handa[1,8] and Toyohiro Hirai[1]

Abstract

Background Little is known about whether central airway morphological changes beyond traction bronchiectasis develop and affect clinical outcomes in patients with idiopathic pulmonary fibrosis (IPF). This study aimed to compare central airway structure comprehensively between patients with IPF, subjects with interstitial lung abnormality (ILA), and those without ILA (control) using computed tomography (CT). We further examined the prognostic impact of IPF-specific CT airway parameters in patients with IPF.

Methods This retrospective study included male patients with IPF, and male health checkup subjects divided into those with ILA and control based on lung cancer screening CT. Using an artificial intelligence-based segmentation technique, the extent of fibrotic regions in the lung was quantified. After airway tree segmentation, CT parameters for central airway morphology, including the lumen area of the extrapulmonary airways (LA^{extra}), wall and lumen area of the segmental/subsegmental intrapulmonary airways (WA^{intra} and LA^{intra}), tracheal distortion (tortuosity and curvature) and bifurcation angle of the main carina, were calculated.

Results There were 106 patients with IPF, 53 subjects with ILA, and 1295 controls. Multivariable models adjusted for age, height and smoking history revealed that LA^{intra} and WA^{intra} were larger in both ILA and IPF, and that tracheal tortuosity and curvature were higher in IPF, but not in ILA, than in the control, whereas the bifurcation angle did not differ between the 3 groups. According to multivariable Cox proportional hazards models including only patients with IPF, increased WA^{intra} was significantly associated with greater mortality (standardized hazard ratio [95% confidence interval] = 1.58 [1.17, 2.14]), independent of the volume of fibrotic regions, normal-appearing regions, or the whole airway tree in the lung.

Conclusion Increased lumen area and wall thickening of the central airways may be involved in the pathogenesis of ILA and IPF, and wall thickening may affect the prognosis of patients with IPF.

*Correspondence:
Naoya Tanabe
ntana@kuhp.kyoto-u.ac.jp

Full list of author information is available at the end of the article

Keywords Idiopathic pulmonary fibrosis, Interstitial lung abnormality, Computed tomography, Imaging, Central airway morphology, Airway disease, Tortuosity, Curvature, Traction bronchiectasis

Background

Idiopathic pulmonary fibrosis (IPF) is a devastating interstitial lung disease (ILD) without established curative treatments. Despite extensive attempts to control disease progression with antifibrotic drugs, the clinical prognosis remains unsatisfactory [1, 2]. In addition to the alveolar epithelium, which is a primary pathological site of IPF [3], a growing body of literature suggests the involvement of cells constituting central and peripheral airways in pulmonary fibrosis [4–6]. Previous studies have focused mainly on traction bronchiectasis in the intrapulmonary central airways visible on computed tomography (CT) and in the peripheral airways on histology, while little is known about the morphological changes in central airways such as the trachea, main bronchi, or segmental bronchi.

Lung parenchyma fibrosis generates traction force and causes bronchial dilation, termed traction bronchiectasis. The high incidence of traction bronchiectasis in IPF suggests that even other morphological changes in the airway may be secondary to pulmonary parenchyma fibrosis in patients with IPF. However, this concept has been challenged by recent studies showing that the number of terminal bronchioles is lower even in local nonfibrotic regions [7, 8] and that airway volume is associated with prognosis independent of changes in the lung parenchyma [9]. It is presumed that airway lesions may develop independently of surrounding fibrosis not only in patients with IPF but also in patients with an early-stage disease that would be subsequently diagnosed as IPF. In the early stage of pulmonary fibrosis, interstitial lung abnormality (ILA), defined as an incidental radiological abnormality suggestive of underlying ILD [10], has been increasingly recognized as a precursor to ILDs, including IPF [11], and the significance of airway lesions in ILA has recently been explored [12]. Therefore, we hypothesized that central airway morphological changes independent of lung parenchyma fibrosis are associated with the pathogenesis of ILD, including IPF.

The purpose of this study was to examine whether the central airways display greater morphological changes on CT in subjects with ILA and IPF than in those without ILA or ILD. Since the wall area, tortuosity and eccentricity of the airways have been reported as airway morphological features in ILD, without detailed analyses of their clinical relevance [12–15], this study comprehensively quantified tortuosity, curvature, torsion, and eccentricity of the trachea; bifurcation angle of the main carina; lumen areas of the extra- and intrapulmonary airways; and wall areas of the intrapulmonary airways in patients with IPF, subjects with ILA and control subjects. The airway parameters that differed between controls and patients with IPF were examined for prognostic impact using follow-up data of patients with IPF.

Methods

Study design

This retrospective study used two different datasets: those of an IPF cohort and a health checkup cohort. The IPF cohort data included all consecutive male patients with IPF who were aged 40 years or older and who underwent CT and spirometry within a period of 3 months during the exacerbation-free period at Kyoto University Hospital between 2011 and 2019. The health checkup cohort data included all consecutive male subjects who were aged 40 years or older who underwent spirometry and lung cancer screening CT in the Japanese medical checkup program during the following periods: 2012–2014 at Kitano Hospital, 2016–2020 at Takeda Hospital, and 2019–2022 at Kyoto Preventive Medical Center. In Japan, subjects in medical checkup programs can voluntarily select an option for lung cancer screening CT regardless of their smoking history. In both cohorts, the exclusion criteria were lack of demographic data and smoking information, inappropriate quality CT images, pleural effusion, pneumothorax and pneumomediastinum. The study was conducted in accordance with the Declaration of Helsinki. The ethics committees of Kyoto University Hospital (R2733-8, R2751-2, R1660-6, R1353, R1323-2) approved the study and waived written informed consent because of its retrospective nature.

Spirometry

Spirometry was conducted without a bronchodilator and was evaluated in each facility by well-trained technicians according to the American Thoracic Society/European Respiratory Society statement [16]. The predicted forced expiratory volume in 1 s (FEV_1) and forced vital capacity (FVC) values were calculated using the LMS (lambda, mu, sigma) method reference equations, taking age, sex and height into account [17]. The diffusing capacity of the lung for carbon monoxide (D_{LCO}) was measured in the IPF cohort, and the predicted values were calculated by the reference equations for the Japanese population [18].

CT acquisition

The entire lungs were scanned at full inspiration using an Aquilion 64, Aquilion ONE, Aquilion PRIME scanner (Canon Medical Systems, Otawara, Japan) and Revolution EVO (GE Healthcare, Chicago, Illinois, USA). The

scanning conditions were 120 kVp and autoexposure control. Images with 0.5 mm/1.25 mm slice thickness were reconstructed with a sharp kernel. Phantom tubes mimicking airways were scanned at all the scanners to validate the accuracy of segmentation. As shown in Supplementary Figure S1, there were no systematic differences in measurement errors between the different CT scanners.

CT analysis

Automatic three-dimensional segmentation of the lung parenchyma and entire airway tree from the original chest CT was performed with SYNAPSE VINCENT software (FUJIFILM, Tokyo, Japan). From the volume of segmented lung parenchyma (Lung volume^{CT}), the percent predicted volume of lung parenchyma (%Lung volume^{CT}) was calculated according to the reference values of the Japanese population [19]. The segmented airway tree was exported as DICOM files and further processed using a custom script implemented in Python 3. To perform the morphological analysis of the airway, images were rescaled to have isotropic 1–1.25 mm voxels for subsequent analyses. The trachea above the level of the aortic arch was automatically removed because the entire trachea was not always included on CT.

Diagnosis of IPF and ILA

The diagnosis of IPF was based on the official ATS/ERS/JRS/ALAT guidelines [20, 21]. As previously reported [22], one chest radiologist and two pulmonologists who were blinded to the patient information visually assessed the chest CT images for ILA according to the Fleischner Society's guidelines [6]. The cases with discordance were judged by a chest radiologist or by consultation with two raters. Subtypes of ILA (non-subpleural, subpleural non-fibrotic, subpleural fibrotic) were also classified.

AIQCT software

Radiological parenchymal and airway abnormalities of the lung parenchyma were automatically segmented and quantified using AI-based image analysis software named AIQCT (Fujifilm Corporation, Tokyo, Japan) [9]. AIQCT uses a network architecture based on U-Net to automatically classify chest CT images into the following types: normal lung, ground-glass opacity, reticulation, consolidation, honeycombing, nodules, hyperlucency, interlobular septum, bronchi, and vessels. The percentage of fibrotic area (% Fibrosis) was defined as the percentage of lung volume occupied by regions with reticulation and honeycombing.

Geometric analysis of the central airway

Automatic three-dimensional segmentation of the entire airway tree from the original chest CT was performed by SYNAPSE VINCENT software (FUJIFILM, Tokyo, Japan). Figure 1A provides an overview of the geometric evaluation of the airway. First, the mean airway lumen and wall areas were measured. To further evaluate the

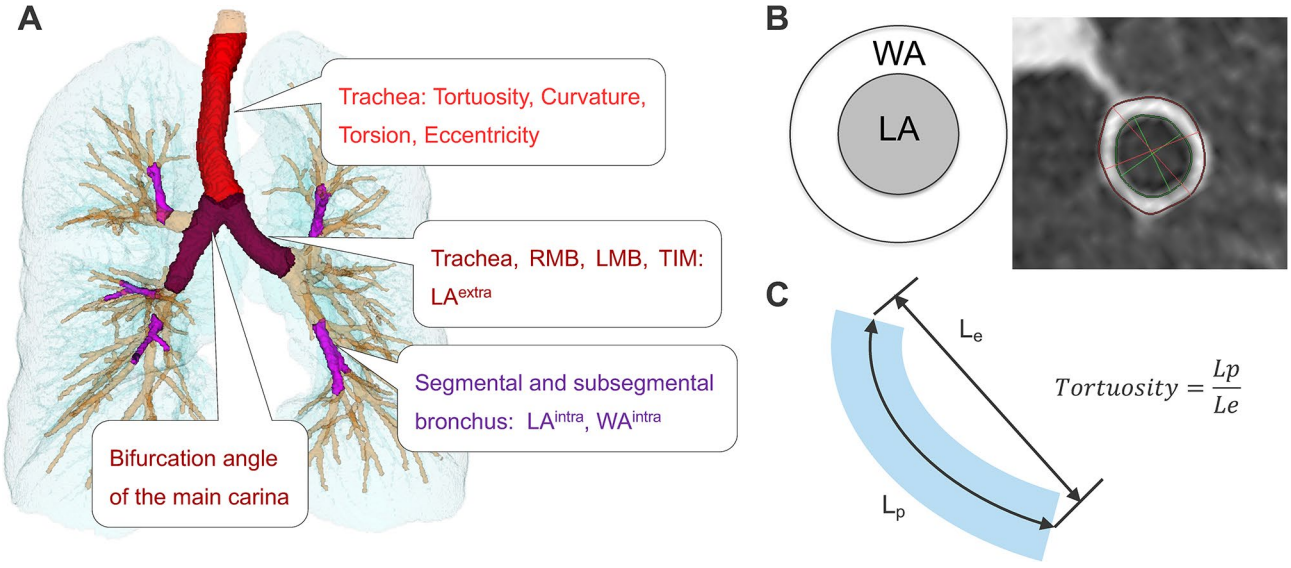

Fig. 1 Airway morphology assessment. **A**. Overview of the geometric evaluation of the airway. Tortuosity, curvature and torsion of the trachea were measured. Mean airway lumen and wall areas were measured from the coloured airway branch. Geometric mean of the extrapulmonary airway lumen area (LA^{extra}) was calculated for trachea, RMB, LMB and TIM. Geometric mean of the intrapulmonary airway lumen area (LA^{intra}) and mean volume of the wall area (WA^{intra}) were calculated for the segmental and subsegmental bronchi. Bifurcation angle of the main carina was also measured. RMB: right main bronchus, LMB: left main bronchus, TIM: truncus intermedius, LA: lumen area WA: wall area. **B**. Measurement of the lumen area and wall area was performed by SYNAPSE VINCENT software based on the full-width half-maximum principle. **C**. Path length (Lp) and Euclidean distance (Le) of the trachea were acquired from the centreline of the airway tree. Tortuosity of the trachea was calculated as the path length divided by the Euclidean distance

geometric properties of the trachea, the following parameters were extracted: tortuosity, curvature, torsion, eccentricity, and bifurcation angle of the main carina. The details of each airway parameter are described below.

Central airway size and wall area assessment

Lumen and wall areas were measured on SYNAPSE VINCENT software. The cross-sectional lumen area (LA) at 14 branch segments, including the trachea, right and left main bronchus (RMB and LMB), bronchus intermedius, and segmental and subsegmental bronchus of 5 paths (RB1, RB4, RB10, LB1, LB10, sRB1, sRB4, sRB10, sLB1 and sLB10), was measured by applying the full-width half maximum principle, as previously reported [23, 24] (Fig. 1A and B). The geometric means of the extrapulmonary airway lumen area (LA^{extra}) and the intrapulmonary airway lumen area (LA^{intra}) were calculated from the geometric mean of each airway area as follows:

- $$LA^{\text{extra}} = \sqrt[4]{LA^{trachea} \times LA^{RMB} \times LA^{LMB} \times LA^{TIM}}$$

- $$LA^{intra} = \sqrt[10]{\begin{matrix} LA^{RB1} \times LA^{RB4} \times LA^{RB10} \times LA^{LB1} \times LA^{LB10} \times \\ LA^{sRB1} \times LA^{sRB4} \times LA^{sRB10} \times LA^{sLB1} \times LA^{sLB10} \end{matrix}}$$

LA: lumen area; RMB: right main bronchus; LMB: left main bronchus; TIM: truncus intermedius.

Wall area (WA) of the segmental and subsegmental airways at the above 10 sites (RB1, RB4, RB10, LB1, LB10, sRB1, sRB4, sRB10, sLB1 and sLB10) was also measured. The geometric mean of these wall areas (WA^{intra}) was calculated.

Tortuosity, curvature, torsion

First, the segmented airway tree was skeletonized to obtain the centreline of the tree. The branching points were localized, and the location of the trachea was automatically identified using the custom Python scripts "Skan" and "ductal_morphology" (from https://github.com/shizuo-kaji/ductal_morphology) [25]. The path length and Euclidean distance of the trachea were acquired from the centreline of the airway tree. Tortuosity of the trachea was calculated as the path length divided by the Euclidean distance (Fig. 1C).

Second, the curvature and torsion of the trachea were calculated (Supplementary Figure S2). Curvature represents two-dimensional steepness of the curve, whereas torsion represents three-dimensional curve twisting. The details of this method are described in Supplementary Figure S2. To compute these measures, ten points along the centreline of the trachea were sampled, and a spline curve was fitted through these points. The overall curvature and torsion were then calculated as the mean values across the ten sampled points. The correlations of torsion and curvature with tortuosity were also evaluated (Supplementary Figure S3).

Eccentricity and bifurcation angle of the main carina

Eccentricity refers to the deviation of the airway's cross-section from a true circle. Eccentricity ranges between 0 and 1, where 0 is the representation of a true circle and a value near 1 represents a very elongated ellipse. A cross-section of the airway perpendicular to the centreline was made at 10 locations, and the mean eccentricity at these cross-sections was used as the eccentricity of the trachea (Supplementary Figure S4). The bifurcation angle of the main carina was calculated by two vectors: vectors from the main carina to the end points of the left and right main bronchi.

Statistical analysis

Values are expressed as the mean±standard deviation (SD) unless otherwise indicated. %Fibrosis and mean torsion of the trachea were log-transformed to follow a normal distribution to run statistical tests other than calculating Spearman's correlation coefficient. The normality of the other parameters was tested. The three groups (checkup cohort with and without ILA and the IPF group) were compared by analysis of variance (ANOVA) followed by Dunnett's post hoc test. Spearman's correlation coefficient (rho) was calculated between airway parameters and %Fibrosis. Multivariable linear regression models were constructed to test whether each CT parameter was associated with ILA or IPF. The models included the presence of ILA or IPF, age, height, and smoking history (current smoking, smoking duration≥20 years and daily tobacco consumption≥1 pack/day) as independent variables, based on previous reports showing the associations of age and sex with airway size [26, 27]. Differences in survival rates according to the median values of each airway parameter were estimated by Kaplan–Meier analysis in the IPF cohort. The log-rank test was also used to compare survival curves between groups. Patients were censored at the time of lung transplantation or the last visit up to 10 years. A Cox proportional hazards model was used to assess the associations between airway parameters and survival. The independent variables of age, height, smoking pack-years, FVC, D_{LCO}, %Fibrosis, airway volume and normal lung volume from AIQCT were selected based on previous reports [9, 20]. Each variable was standardized for multivariable linear regression models and Cox proportional hazards models. Statistical analyses were performed using R statistical software version 4.1.0.

Table 1 Patient characteristics

	ILA - (Control)	ILA +	IPF	*p*
n	1295	53	106	
Age	56.8 (10.2)	67.7 (8.2)	71.4 (8.7)	< 0.001
Sex, male, n(%)	1295 (100.0)	53 (100.0)	106 (100.0)	
Height, cm	170.3 (6.0)	168.7 (7.4)	165.7 (6.0)	< 0.001
Weight, kg	70.4 (10.7)	68.7 (9.5)	67.5 (10.7)	0.017
Current smoker, n(%)	500 (38.6)	21 (39.6)	6 (5.7)	< 0.001
Former smoker, n(%)	405 (31.3)	23 (43.4)	94 (88.7)	< 0.001
Smoking pack-years	NA	NA	46.6 (33.0)	
Smoking duration, ≥ 20 years, n(%)	761 (58.8)	40 (75.5)	92 (86.8)	< 0.001
Daily tobacco consumption, ≥ 1 pack/day, n(%)	501 (38.7)	31 (58.5)	83 (78.3)	< 0.001
%FEV_1	95.1 (14.6)	91.8 (14.8)	87.2 (16.1)	< 0.001
%FVC	97.5 (12.7)	94.5 (14.1)	82.3 (17.8)	< 0.001
FEV_1/FVC	0.77 (0.07)	0.75 (0.08)	0.82 (0.08)	< 0.001
$\%D_{LCO}$	NA	NA	46.1 (14.8)	
Lung Volume^{CT}, L	5248 (922)	4842 (860)	3684 (877)	< 0.001
%Lung Volume^{CT}	105.4 (16.2)	102.0 (16.2)	81.6 (18.0)	< 0.001
%Fibrosis	0.10 [0.04, 0.25]	0.81 [0.43, 1.91]	6.50 [4.04, 11.38]	< 0.001

Patient characteristics of the three groups: ILA- (health checkup cohort without ILA), ILA+ (health checkup cohort with ILA), and IPF. Data are expressed as mean (SD) or n (%). %Fibrosis is expressed as median [interquartile range], although statistical analysis was performed after log transformation to make this variable follow a normal distribution. Comparisons of the three groups were performed by analysis of variance (ANOVA). Asterisk (*) means $\%D_{LCO}$ was measured only in IPF and could not be measured in two patients ($n=104$). FEV_1: forced expiratory volume in 1 s, FVC: forced vital capacity, D_{LCO}: diffusing capacity of the lung for carbon monoxide, %Lung Volume^{CT}: the percent predicted volume of lung parenchyma (lung volume divided by the reference value)

Table 2 Differences in all airway parameters between ILA-, ILA + and IPF groups

	ILA - (Control)	ILA +	IPF	*p*
LA^{extra}, mm^2	190.3 (33.4)	194.3 (33.4)	217.9 (46.9)***	< 0.001
LA^{intra}, mm^2	16.6 (4.7)	18.6 (5.0)**	20.6 (5.4)***	< 0.001
WA^{intra}, mm^2	46.0 (8.3)	51.0 (9.5)***	61.7 (9.7)***	< 0.001
Tortuosity	1.18 (0.03)	1.18 (0.03)	1.19 (0.04)***	< 0.001
Curvature	0.10 (0.05)	0.10 (0.04)	0.12 (0.05)**	0.003
Torsion	0.40 [0.26, 0.61]	0.48 [0.29, 0.64]	0.42 [0.28, 0.59]	0.64
Eccentricity	0.53 (0.09)	0.55 (0.10)	0.55 (0.10)	0.013
Bifurcation angle	95.3 (10.2)	93.3 (9.3)	93.6 (12.1)	0.11

Data are expressed as mean (SD) or n (%). Torsion is expressed as median [interquartile range], although statistical analysis was performed after log transformation to make this variable follow a normal distribution. P value indicates a difference between three groups according to ANOVA (analysis of variance). Asterisks (*) indicate significant differences according to Dunnett's post hoc test; ** $p<0.01$, *** $p<0.001$

Results

Of the 108 patients with IPF, 2 were excluded due to unsuitable CT images, and 106 patients were included. Of the 1381 health checkup subjects, 33 were excluded due to lack of demographic data, inappropriate CT images or pneumothorax, and 1348 were included (Supplementary Figure S5).

Based on the presence of ILA, 1348 health checkup subjects were divided into those with ILA ($n=53$, 3.9%) and those without ILA (control, $n=1295$, 96.1%). Table 1 describes the characteristics of the control, ILA, and IPF groups. There was no significant difference in %Lung volume between the control and ILA. The ILA and IPF groups had higher proportions of former smokers. Among cases of ILA, the most common type was subpleural fibrotic type ($n=26$, 49.1%), followed by subpleural non-fibrotic type ($n=24$, 45.3%) and non-subpleural type ($n=3$, 5.7%).

As shown in Table 2, LA^{extra} was larger in IPF, and LA^{intra} and WA^{intra} were larger in ILA and IPF than in the control. Tortuosity and curvature of the trachea were significantly higher in IPF, but not in ILA. Tracheal eccentricity was higher in both ILA and IPF. There were no significant differences in tracheal torsion or the bifurcation angle of the carina between the groups. The trends for LA^{extra}, LA^{intra}, WA^{intra}, tortuosity, curvature, and torsion are shown in Fig. 2.

Table 3 shows that in the multivariable models, LA^{intra} and WA^{intra} were larger in ILA and IPF than in the control after adjusting for age, height and smoking history. Moreover, LA^{extra} was larger and tortuosity and curvature were higher in IPF than in the control. Similar results were obtained when subjects suspected of other airway diseases (asthma, COPD, combined pulmonary fibrosis and emphysema (CPFE)) were excluded, when the subjects were limited to those with a history of smoking, or when the health checkup cohort was divided into subjects with and without subpleural fibrotic ILA (Supplementary Table S1 & S2 & S3).

Figure 3 shows the associations between %Fibrosis and airway parameters. WA^{intra} was associated with %Fibrosis in ILA and IPF (rho=0.35, $p=0.01$, and rho=0.31, $p=0.001$, respectively). LA^{extra} was associated with %Fibrosis in IPF (rho=0.23, $p=0.02$).

Moreover, the associations of airway parameters with mortality in IPF were examined. The log-rank test showed that WA^{intra} was associated with mortality, but the other airway parameters were not (Fig. 4). A Cox proportional hazards model revealed that increased WA^{intra} was associated with mortality when adjusted for age, height, smoking pack-years, FVC, D_{LCO}, %Fibrosis, normal lung volume, and airway volume (Table 4).

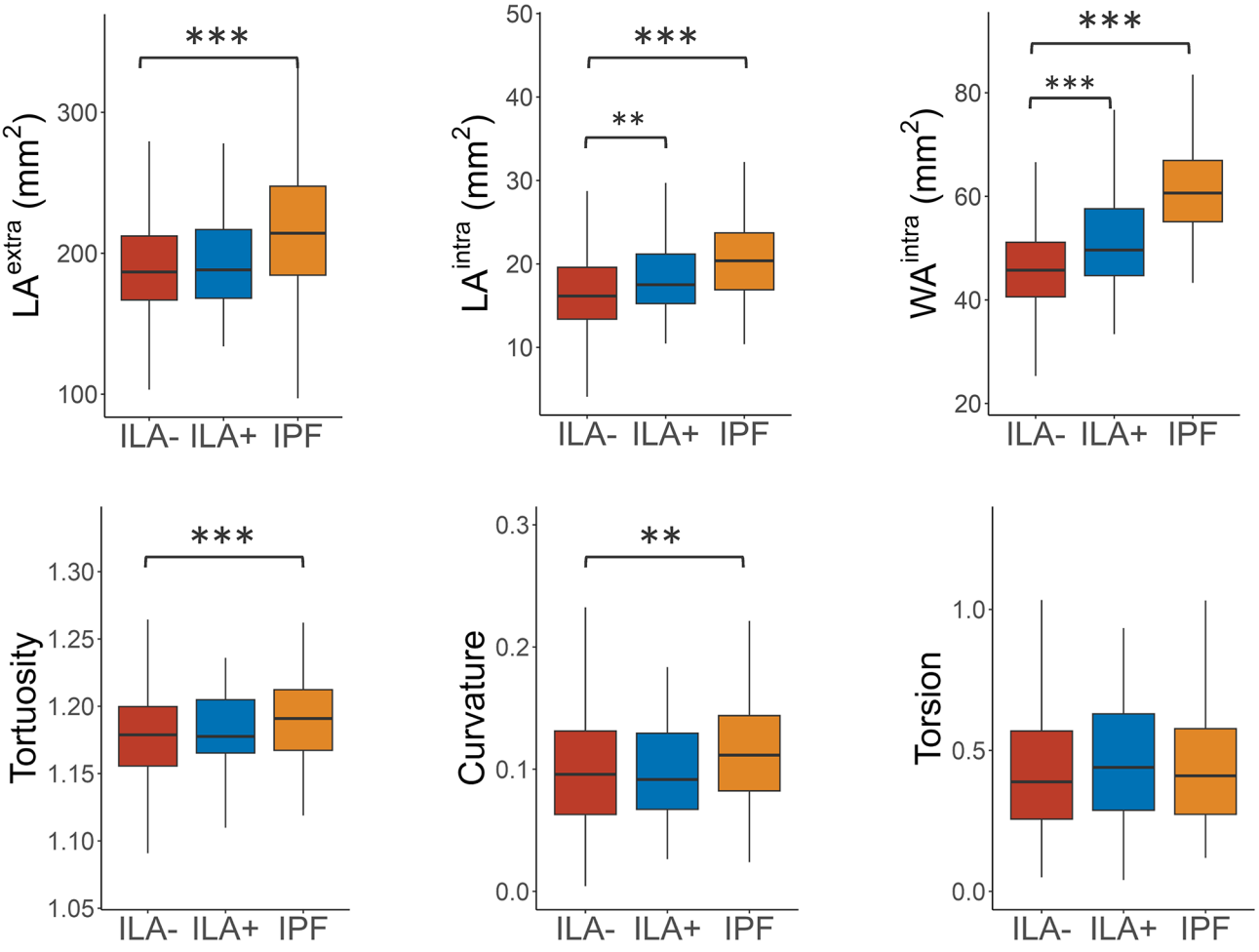

Fig. 2 Distributions of and differences in representative airway parameters between ILA-, ILA + and IPF. Asterisks (*) indicate significant differences by Dunnett's post hoc test; ** $p < 0.01$, *** $p < 0.001$

Table 3 Multivariable analysis of differences in airway parameters between ILA-, ILA + and IPF groups

	ILA - (Control)	ILA +	IPF
LA^{extra}	Ref	0.03 [-0.24, 0.29]	0.72 [0.51, 0.93]***
LA^{intra}	Ref	0.34 [0.07, 0.61]*	0.91 [0.70, 1.12]***
WA^{intra}	Ref	0.36 [0.11, 0.60]**	1.58 [1.38, 1.77]***
Tortuosity	Ref	0.03 [-0.25, 0.31]	0.26 [0.04, 0.48]*
Curvature	Ref	-0.14 [-0.41, 0.14]	0.36 [0.14, 0.58]**

The association between each airway parameter and the presence of ILA or IPF was evaluated in multivariable regression models. Models were adjusted for age, height and smoking history (current smoking, smoking duration and daily tobacco consumption). Values are expressed as standardized estimate [95% confidence interval]. Significant differences are indicated as follows: * $p < 0.05$, ** $p < 0.01$, *** $p < 0.001$

Discussion

This study showed that LA^{intra} and WA^{intra} were larger in ILA and IPF than in the control even after adjustment for age, height and smoking history. LA^{extra}, tortuosity and curvature were greater in IPF than in the control, with no significant difference between control and ILA. While WA^{intra} was weakly associated with %Fibrosis, survival analyses in patients with IPF showed that a larger WA^{intra} was associated with higher mortality independent of %Fibrosis, normal lung volume, and airway volume. This is the first study to compare various central airway morphologies in patients with ILA and IPF relative to control and to explore the prognostic impact of larger wall areas in patients with IPF. Our data support the recent hypothesis that in addition to lung parenchymal fibrosis, airway diseases may also be involved in the pathogenesis of IPF.

The larger LA^{intra} and WA^{intra} in both ILA and IPF and their absence or weak correlations with %Fibrosis suggest that the size of the lumen and wall areas of the intrapulmonary central airways cannot be explained solely by the surrounding fibrosis and traction bronchiectasis. We postulate the following two mechanisms. First, the enlargement of lumen and wall areas of the central airways develops in the early stage of IPF. This would be consistent with recent reports on the involvement of the airway epithelium in the fibrotic process in ILD [6, 28]. Second, the larger lumen and wall of central airways may be native structures that increase susceptibility to lung

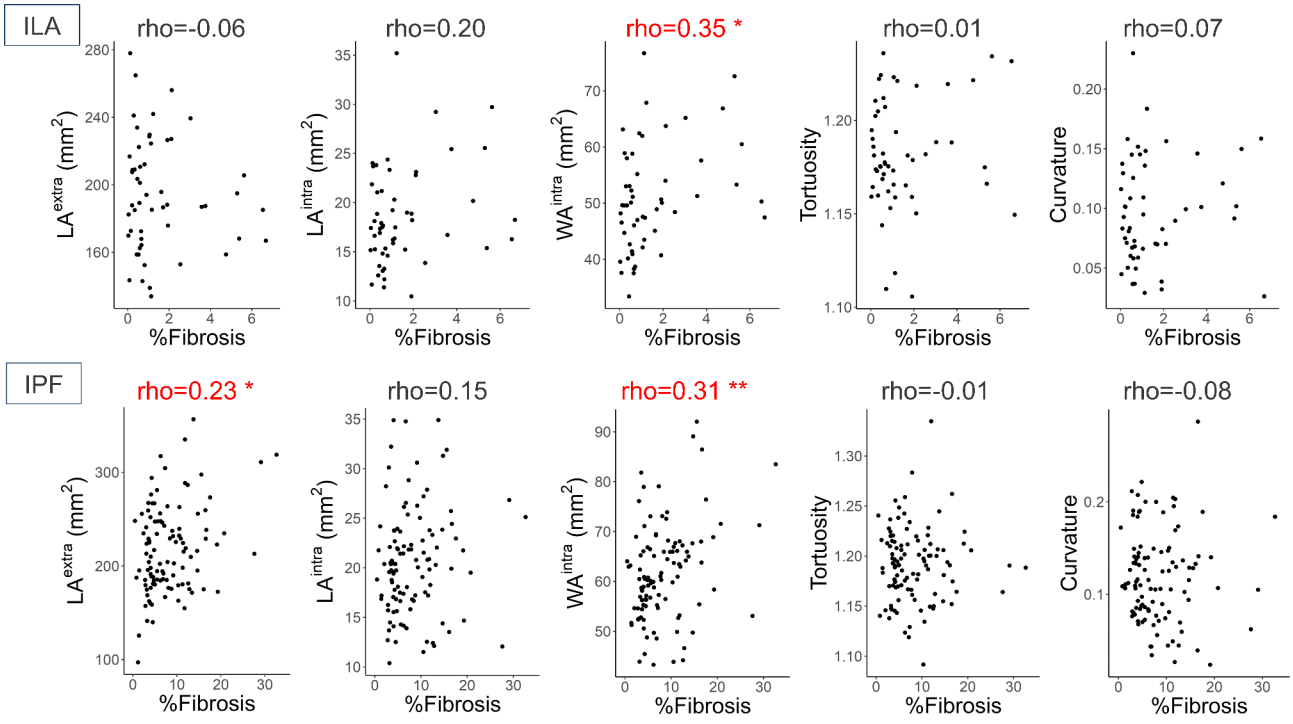

Fig. 3 Associations between %Fibrosis and airway parameters. Spearman's correlation coefficient (rho) is shown in each graph, and its significance is indicated as follows: * $p < 0.05$, ** $p < 0.01$

fibrosis and promote IPF development. This concept is in line with the previous finding that a smaller airway size for a given lung size (dysanapsis) is associated with lower pulmonary function in healthy subjects and future development of chronic obstructive pulmonary disease (COPD) [23, 24, 29], although the directionality is opposite with IPF and COPD. Demographic factors such as age, sex, and body size cannot fully explain the wide variation in airway dimensions in healthy subjects [26]. Moreover, genetic factors such as fibroblast growth factor 10 (FGF10) or FGF18, which are factors associated with lung fibrosis [30, 31], can also affect native airway structure [32, 33]. Further studies are needed to clarify whether healthy individuals who carry genetic factors associated with native airway structure exhibit larger relative airway sizes and more frequently develop IPF.

The larger WA^{intra} in both ILA and IPF and the prognostic impact of larger WA^{intra} independent of %Fibrosis in IPF are the main findings of this study. This finding is consistent with previous reports on thickening of the airway wall in ILD or ILA [8, 34]. An increase in airway wall thickness has been correlated with reductions in lung volume in some ILA populations [12]. Together with the observed weak association between WA^{intra} and %Fibrosis in ILA and IPF, we speculate that airway wall thickening may progress in parallel with the progression of lung fibrosis in ILD. Furthermore, our log-rank test and Cox proportional hazard models showed a significant association between airway wall thickening and prognosis, independent of lung parenchymal abnormalities, airway volume, or pulmonary function test results. Although the underlying mechanism is unclear, airway wall thickening may be an independent prognostic factor. Various airway lesions in peripheral lung tissues have been reported in IPF, including inflammatory cell infiltration and peribronchiolar fibrosis leading to airway wall thickening [4, 5], but very few reports have focused on pathologic changes in the central airway. Thus, further studies using relatively large lung tissue samples including the central airways are needed to explore what histological features could be represented by a CT finding of increased wall area of the segmental and subsegmental airways in patients with IPF.

The greater tortuosity and curvature of the trachea observed in IPF are consistent with previous reports on the associations between ILD and airway lumen distortion [13, 14]. However, the lack of associations between these airway parameters and mortality is not consistent with the study by Cheung et al., who reported that segmental tortuosity was associated with IPF mortality [14]. Our study and the study by Silva BRA et al. [13] measured the tortuosity of the trachea, whereas Cheung et al. [14] measured the tortuosity of airway generation 2–6. The different locations of the airways used for measuring tortuosity might have caused the discordant results. Interestingly, such geometric morphological changes

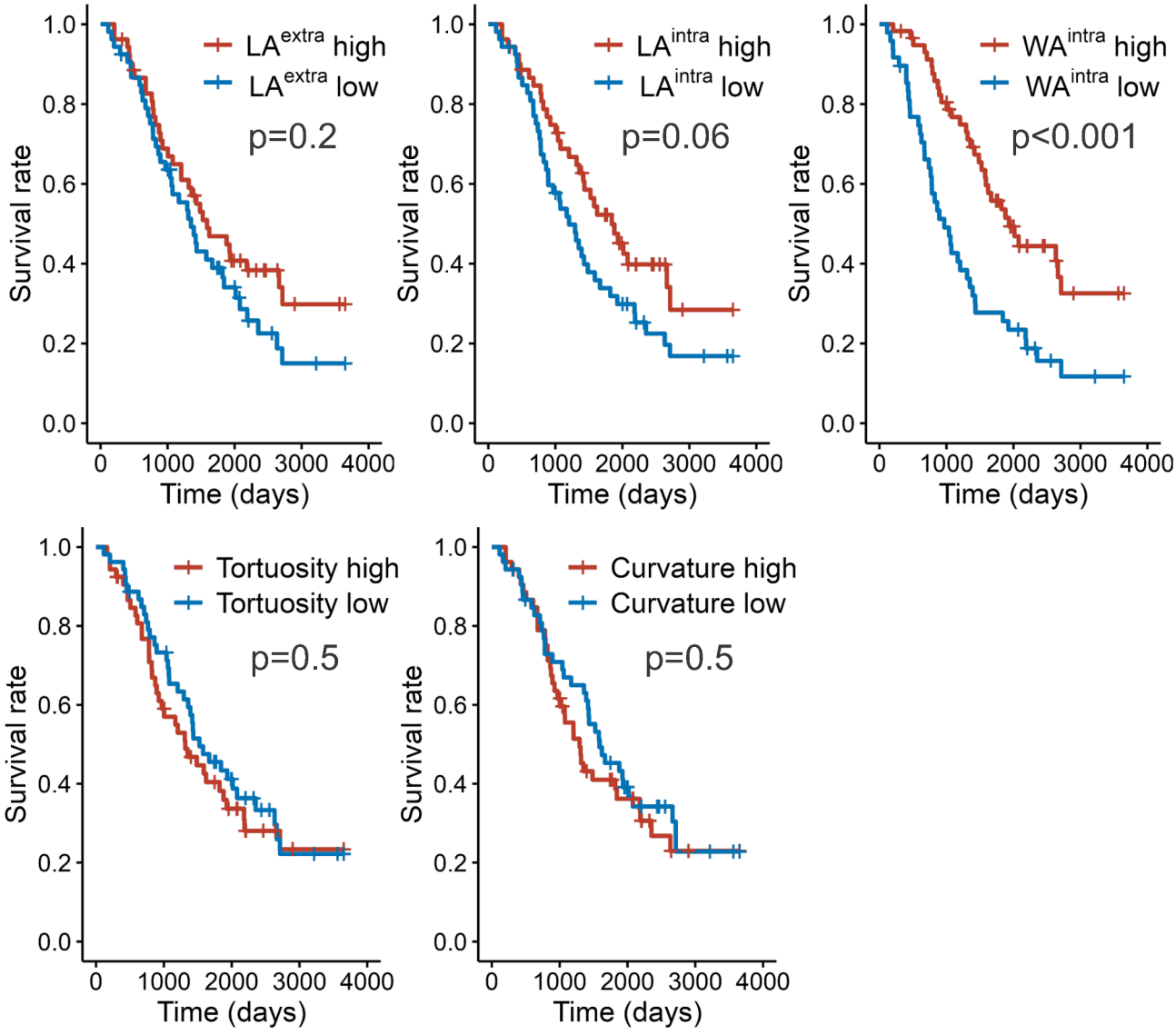

Fig. 4 Survival curves for airway parameters, Differences in survival rates according to the median values of each airway parameter were estimated via Kaplan–Meier analysis in IPF cohort. The log-rank test was also used to compare survival curves between groups

can be observed even in tracheas where the influence of traction bronchiectasis is not apparent. Moreover, since tortuosity and curvature were not significantly different between ILA and the control, those changes are presumably features of progressed IPF rather than early-stage IPF. In this study, tortuosity and curvature were related to IPF, but torsion showed no relationship. Furthermore, the correlation between curvature and tortuosity was stronger than the correlation between torsion and tortuosity. Mathematically, curvature and torsion are important metrics in the evaluation of curves since two curves are congruent when they have the same curvature and torsion. Theoretically, both high curvature and high torsion should lead to high tortuosity, but increased tracheal tortuosity in IPF can be ascribed mainly to curvature, two-dimensional steepness differences in the trachea. Difference in the correlations of these two parameters with tortuosity, and different results of these two parameters in IPF and the control, imply that both curvature and torsion need to be considered when evaluating the geometric properties of the central airway.

No significant differences in tracheal eccentricity or the bifurcation angle of the main carina were found between patients with ILA or IPF and control. Airway eccentricity has also been analysed as a morphological marker of the airway [15]. The eccentricity of the airway was elevated in ILD and COPD, which may indicate the presence of airway lesions [13, 35]. The bifurcation angle of the main carina has been widely used to assess the morphological features of the airway. The bifurcation angle is not

Table 4 Multivariable cox proportional hazard model for the association with survival

	Standardized hazard ratio [95%CI]			
	Model 1	**Model 2**	**Model 3**	**Model 4**
Age	1.25 [0.87, 1.8]	1.26 [0.87, 1.83]	1.35 [0.93, 1.96]	1.36 [0.93, 1.98]
Height	0.9 [0.61, 1.32]	0.91 [0.62, 1.34]	1.01 [0.7, 1.47]	0.98 [0.67, 1.43]
Pack-years	1.13 [0.84, 1.51]	1.12 [0.84, 1.51]	1.15 [0.87, 1.51]	1.15 [0.88, 1.52]
FVC	0.94 [0.65, 1.35]	0.94 [0.65, 1.36]	1.12 [0.77, 1.64]	1.12 [0.77, 1.63]
D_{LCO}	0.63[0.42, 0.96]*	0.62[0.4, 0.96]*	0.59[0.41, 0.86]**	0.64[0.42, 0.98]*
%Fibrosis	1.52[1.04, 2.23]*	1.57[1.02, 2.41]*		
Airway		0.93 [0.59, 1.47]		1.15 [0.78, 1.69]
Normal Lung			0.54[0.35, 0.83]**	0.54[0.35, 0.84]**
WA^{intra}	1.58[1.17, 2.14]**	1.63[1.13, 2.34]**	1.5[1.11, 2.02]**	1.41[1, 1.99]*
(C-index in each model)	0.78	0.78	0.78	0.79

A Cox proportional hazards model was used to assess the association between WA^{intra} and survival in IPF. Independent variables were selected from age, FVC, D_{LCO}, %Fibrosis, airway volume and normal lung volume from AIQCT. Two patients were excluded from this analysis ($n=104$) due to a lack of D_{LCO} data. Values are expressed as standardized hazard ratio [95% confidence interval]. Significant differences are indicated as follows: * $p<0.05$, ** $p<0.01$. FVC: forced vital capacity, D_{LCO}: diffusing capacity of the lung for carbon monoxide

affected by age, sex, or body size [36, 37] and can influence air velocity or particle deposition [38, 39]. However, as our data did not show an association between these two parameters and ILA or IPF, the bifurcation angle and eccentricity may not be factors characterizing airway morphology in IPF.

There are several limitations to this study. First, due to the small number of female subjects with ILA or IPF, only males were included. Second, this study was conducted only in the Japanese population. Given that ethnicity affects airway morphology, the present results need to be confirmed in other populations. Third, multiple CT scanners with different conditions were used, which may have affected the results. Despite the systematic error of the overestimation of wall area in CT measurements [40], we believe that the impact of different CT scanners was small because the extent of measurement errors did not differ between the scanners, and the analysis was performed in the central airway. Fourth, because of the lack of information about the total amount of smoking in the health checkup cohort, smoking duration ≥ 20 years and daily tobacco consumption ≥ 1 pack/day were used in the multivariable analysis.

In conclusion, the central airway lumen area and airway wall area were larger in IPF and ILA. Their associations with lung fibrosis were weak, and a larger wall area was associated with higher mortality independent of lung fibrosis in patients with IPF. Therefore, wall thickening of the central airways can develop even in subjects with ILA and subsequently becomes an important prognostic factor in patients with IPF.

Abbreviations

IPF	Idiopathic Pulmonary Fibrosis
ILD	Interstitial Lung Disease
ILA	Interstitial Lung Abnormality
CT	Computed Tomography
LA^{extra}	Lumen Area of the Extrapulmonary Airways
LA^{intra}	Lumen Area of the Segmental/Subsegmental Intrapulmonary Airways
WA^{intra}	Wall Area of the Segmental/Subsegmental Intrapulmonary Airways
FEV_1	Forced Expiratory Volume in 1 s
FVC	Forced Vital Capacity
D_{LCO}	Diffusing Capacity of the Lung for Carbon Monoxide
SD	Standard Deviation
ANOVA	Analysis of Variance
CPFE	Combined Pulmonary Fibrosis and Emphysema
COPD	Chronic Obstructive Pulmonary Disease
FGF	Fibroblast Growth Factor

Supplementary Information

The online version contains supplementary material available at https://doi.org/10.1186/s12931-024-03032-5.

Supplementary Material 1

Acknowledgements

The authors would like to thank all the physicians who contributed to the clinical data collection.

Author contributions

TM, NT, KT, SS, T. Handa and T. Hirai were involved in the study design and data interpretation. TM, NT, RS, YS, YH and SK were involved in the CT data analysis. KT, MU, AM, KS, IM, MF and T. Handa were involved in clinical data collection. All authors critically revised the report, commented on drafts of the manuscript, and approved the final report.

Funding

This study was partially supported by a grant from the Japan Society for the Promotion of Science (JSPS) (Grants-in-Aid for Scientific Research 19K08624).

Data availability

The datasets used and/or analysed during the current study are available from the corresponding author upon reasonable request.

Declarations

Ethics approval and consent to participate

The study was conducted in accordance with the Declaration of Helsinki. The ethics committees of Kyoto University Hospital (R2733-8, R2751-2, R1660-6, R1353, R1323-2) approved the study and waived written informed consent because of its retrospective nature.

Consent for publication
Not applicable.

Competing interests
NT, T. Handa, and T. Hirai were supported by grants from FUJIFILM Co., Ltd., and Daiichi Sankyo Company, Ltd. T. Handa is employed by the Collaborative Research Laboratory funded by Teijin Pharma Co., Ltd. SS received grants from FUJIFILM Co., Ltd., Nippon Boehringer Ingelheim, Philips-Respironics, Fukuda Denshi, Fukuda Lifetec Keiji, and ResMed outside of the submitted work. None of these companies played a role in the design or analysis of the study or in the writing of the manuscript. The other authors have no conflicts of interest to declare.

Author details
[1]Department of Respiratory Medicine, Graduate School of Medicine, Kyoto University, 54 Kawahara-cho, Shogoin, Sakyo-ku, Kyoto 606-8507, Japan
[2]Department of Diagnostic Imaging and Nuclear Medicine, Graduate School of Medicine, Kyoto University, 54 Kawahara-cho, Shogoin, Sakyo-ku, Kyoto 606-8507, Japan
[3]Department of Respiratory Care and Sleep Control Medicine, Graduate School of Medicine, Kyoto University, 54 Kawahara-cho, Shogoin, Sakyo-ku, Kyoto 606-8507, Japan
[4]Kyoto Preventive Medical Center, 28 Nishinokyo-Samaryocho, Nakagyo-ku, Kyoto 604-8491, Japan
[5]Medical Examination Center, Takeda Hospital, 277 Aburanokoji-cho, Shimogyo-ku, Kyoto 600-8231, Japan
[6]Respiratory Disease Center, Medical Research Institute Kitano Hospital, PIIF Tazuke- kofukai, 2-4-20 Ohgimachi, Kita-ku, Osaka 530-8480, Japan
[7]Institute of Mathematics for Industry, Kyushu University, 744 Motooka, Nishi-ku, Fukuoka 819-0395, Japan
[8]Department of Advanced Medicine for Respiratory Failure, Graduate School of Medicine, Kyoto University, 54 Kawahara-cho, Shogoin, Sakyo-ku, Kyoto 606-8507, Japan

Received: 27 June 2024 / Accepted: 31 October 2024
Published online: 10 November 2024

References

1. Richeldi L, du Bois RM, Raghu G, Azuma A, Brown KK, Costabel U, Cottin V, Flaherty KR, Hansell DM, Inoue Y, et al. Efficacy and safety of nintedanib in idiopathic pulmonary fibrosis. N Engl J Med. 2014;370:2071–82.
2. Trachalaki A, Sultana N, Wells AU. An update on current and emerging drug treatments for idiopathic pulmonary fibrosis. Expert Opin Pharmacother. 2023;24:1125–42.
3. Lederer DJ, Martinez FJ. Idiopathic pulmonary fibrosis. N Engl J Med. 2018;378:1811–23.
4. Fulmer JD, Roberts WC, von Gal ER, Crystal RG. Small airways in idiopathic pulmonary fibrosis. Comparison of morphologic and physiologic observations. J Clin Invest. 1977;60:595–610.
5. Figueira de Mello GC, Ribeiro Carvalho CR, Adib Kairalla R, Nascimento Saldiva PH, Fernezlian S, Ferraz Silva LF, Dolhnikoff M, Mauad T. Small airway remodeling in idiopathic interstitial pneumonias: a pathological study. Respiration. 2010;79:322–32.
6. Jaeger B, Schupp JC, Plappert L, Terwolbeck O, Artysh N, Kayser G, Engelhard P, Adams TS, Zweigerdt R, Kempf H, et al. Airway basal cells show a dedifferentiated KRT17(high)phenotype and promote fibrosis in idiopathic pulmonary fibrosis. Nat Commun. 2022;13:5637.
7. Tanabe N, McDonough JE, Vasilescu DM, Ikezoe K, Verleden SE, Xu F, Wuyts WA, Vanaudenaerde BM, Colby TV, Hogg JC. Pathology of Idiopathic Pulmonary Fibrosis assessed by a combination of Microcomputed Tomography, Histology, and immunohistochemistry. Am J Pathol. 2020;190:2427–35.
8. Ikezoe K, Hackett TL, Peterson S, Prins D, Hague CJ, Murphy D, LeDoux S, Chu F, Xu F, Cooper JD, et al. Small Airway reduction and fibrosis is an early pathologic feature of idiopathic pulmonary fibrosis. Am J Respir Crit Care Med. 2021;204:1048–59.
9. Handa T, Tanizawa K, Oguma T, Uozumi R, Watanabe K, Tanabe N, Niwamoto T, Shima H, Mori R, Nobashi TW et al. Novel Artificial Intelligence-based technology for chest computed Tomography Analysis of Idiopathic Pulmonary Fibrosis. Ann Am Thorac Soc 2021.
10. Hatabu H, Hunninghake GM, Richeldi L, Brown KK, Wells AU, Remy-Jardin M, Verschakelen J, Nicholson AG, Beasley MB, Christiani DC, et al. Interstitial lung abnormalities detected incidentally on CT: a position paper from the Fleischner Society. Lancet Respiratory Med. 2020;8:726–37.
11. Putman RK, Gudmundsson G, Axelsson GT, Hida T, Honda O, Araki T, Yanagawa M, Nishino M, Miller ER, Eiriksdottir G, et al. Imaging Patterns Are Associated with interstitial lung abnormality progression and mortality. Am J Respir Crit Care Med. 2019;200:175–83.
12. Miller ER, Putman RK, Diaz AA, Xu H, San Jose Estepar R, Araki T, Nishino M, Poli de Frias S, Hida T, Ross J, et al. Increased Airway Wall Thickness in interstitial lung abnormalities and idiopathic pulmonary fibrosis. Ann Am Thorac Soc. 2019;16:447–54.
13. Silva BRA, Rodrigues RS, Rufino R, Costa CH, Vilela VS, Levy RA, Guimaraes ARM, Carvalho ARS, Lopes AJ. Computed tomography trachea volumetry in patients with scleroderma: Association with clinical and functional findings. PLoS ONE. 2018;13:e0200754.
14. Cheung WK, Pakzad A, Mogulkoc N, Needleman S, Rangelov B, Gudmundsson E, Zhao A, Abbas M, McLaverty D, Asimakopoulos D, et al. Automated airway quantification associates with mortality in idiopathic pulmonary fibrosis. Eur Radiol. 2023;33:8228–38.
15. Oakes JM, Scadeng M, Breen EC, Marsden AL, Darquenne C. Rat airway morphometry measured from in situ MRI-based geometric models. J Appl Physiol (1985). 2012;112:1921–31.
16. Miller MR, Hankinson J, Brusasco V, Burgos F, Casaburi R, Coates A, Crapo R, Enright P, van der Grinten CP, Gustafsson P, et al. Standardisation of spirometry. Eur Respir J. 2005;26:319–38.
17. Kubota M, Kobayashi H, Quanjer PH, Omori H, Tatsumi K, Kanazawa M, Clinical Pulmonary Functions Committee of the Japanese Respiratory S. Reference values for spirometry, including vital capacity, in Japanese adults calculated with the LMS method and compared with previous values. Respir Investig. 2014;52:242–50.
18. Nishida S, Kambe M, Sewake N, Takano M, Kawane H. [Pulmonary function in healthy subjects and its prediction. 5. Pulmonary diffusing capacity in adults (author's transl)]. Rinsho Byori. 1976;24:941–7.
19. Tanabe N, Sato S, Shimada T, Kaji S, Shiraishi Y, Terada S, Maetani T, Mochizuki F, Shimizu K, Suzuki M, et al. A reference equation for lung volume on computed tomography in Japanese middle-aged and elderly adults. Respir Investig. 2024;62:121–7.
20. Raghu G, Collard HR, Egan JJ, Martinez FJ, Behr J, Brown KK, Colby TV, Cordier JF, Flaherty KR, Lasky JA, et al. An official ATS/ERS/JRS/ALAT statement: idiopathic pulmonary fibrosis: evidence-based guidelines for diagnosis and management. Am J Respir Crit Care Med. 2011;183:788–824.
21. Raghu G, Remy-Jardin M, Myers JL, Richeldi L, Ryerson CJ, Lederer DJ, Behr J, Cottin V, Danoff SK, Morell F, et al. Diagnosis of idiopathic pulmonary fibrosis. An Official ATS/ERS/JRS/ALAT Clinical Practice Guideline. Am J Respir Crit Care Med. 2018;198:e44–68.
22. Shiraishi Y, Tanabe N, Sakamoto R, Maetani T, Kaji S, Shima H, Terada S, Terada K, Ikezoe K, Tanizawa K, et al. Longitudinal assessment of interstitial lung abnormalities on CT in patients with COPD using artificial intelligence-based segmentation: a prospective observational study. BMC Pulm Med. 2024;24:200.
23. Smith BM, Kirby M, Hoffman EA, Kronmal RA, Aaron SD, Allen NB, Bertoni A, Coxson HO, Cooper C, Couper DJ, et al. Association of Dysanapsis with Chronic Obstructive Pulmonary Disease among older adults. JAMA. 2020;323:2268–80.
24. Maetani T, Tanabe N, Terada S, Shiraishi Y, Shima H, Kaji S, Sakamoto R, Oguma T, Sato S, Masuda I, Hirai T. Physiological impacts of computed tomography airway dysanapsis, fractal dimension, and branch count in asymptomatic never smokers. J Appl Physiol (1985). 2023;134:20–7.
25. Kaji S, Tanabe N, Maetani T, Shiraishi Y, Sakamoto R, Oguma T, Suzuki K, Terada K, Fukui M, Muro S, et al. Quantification of airway structures by persistent homology. IEEE Trans Med Imaging. 2024;43:2758–68.
26. Terada S, Tanabe N, Maetani T, Shiraishi Y, Sakamoto R, Shima H, Oguma T, Sato A, Kanasaki M, Masuda I, et al. Association of age with computed tomography airway tree morphology in male and female never smokers without lung disease history. Respir Med. 2023;214:107278.
27. Matsuoka S, Uchiyama K, Shima H, Ueno N, Oish S, Nojiri Y. Bronchoarterial ratio and bronchial wall thickness on high-resolution CT in asymptomatic subjects: correlation with age and smoking. AJR Am J Roentgenol. 2003;180:513–8.
28. Hancock LA, Hennessy CE, Solomon GM, Dobrinskikh E, Estrella A, Hara N, Hill DB, Kissner WJ, Markovetz MR, Grove Villalon DE, et al. Muc5b overexpression

causes mucociliary dysfunction and enhances lung fibrosis in mice. Nat Commun. 2018;9:5363.
29. Vameghestahbanati M, Hiura GT, Barr RG, Sieren JC, Smith BM, Hoffman EA. CT-Assessed dysanapsis and airflow obstruction in early and Mid Adulthood. Chest. 2022;161:389–91.
30. Yuan T, Volckaert T, Chanda D, Thannickal VJ, De Langhe SP. Fgf10 Signaling in Lung Development, Homeostasis, Disease, and Repair after Injury. Front Genet. 2018;9:418.
31. Joannes A, Brayer S, Besnard V, Marchal-Somme J, Jaillet M, Mordant P, Mal H, Borie R, Crestani B, Mailleux AA. FGF9 and FGF18 in idiopathic pulmonary fibrosis promote survival and migration and inhibit myofibroblast differentiation of human lung fibroblasts in vitro. Am J Physiol Lung Cell Mol Physiol. 2016;310:L615–629.
32. Tang N, Marshall WF, McMahon M, Metzger RJ, Martin GR. Control of mitotic spindle angle by the RAS-regulated ERK1/2 pathway determines lung tube shape. Science. 2011;333:342–5.
33. Whitsett JA, Clark JC, Picard L, Tichelaar JW, Wert SE, Itoh N, Perl AK, Stahlman MT. Fibroblast growth factor 18 influences proximal programming during lung morphogenesis. J Biol Chem. 2002;277:22743–9.
34. Verleden SE, Tanabe N, McDonough JE, Vasilescu DM, Xu F, Wuyts WA, Piloni D, De Sadeleer L, Willems S, Mai C, et al. Small airways pathology in idiopathic pulmonary fibrosis: a retrospective cohort study. Lancet Respir Med. 2020;8:573–84.
35. Ortiz-Puerta D, Diaz O, Retamal J, Hurtado DE. Morphometric analysis of airways in pre-COPD and mild COPD lungs using continuous surface representations of the bronchial lumen. Front Bioeng Biotechnol. 2023;11:1271760.
36. Szelloe P, Weiss M, Schraner T, Dave MH. Lower airway dimensions in pediatric patients-A computed tomography study. Paediatr Anaesth. 2017;27:1043–9.
37. Christou S, Chatziathanasiou T, Angeli S, Koullapis P, Stylianou F, Sznitman J, Guo HH, Kassinos SC. Anatomical variability in the upper tracheobronchial tree: sex-based differences and implications for personalized inhalation therapies. J Appl Physiol (1985). 2021;130:678–707.
38. Zierenberg JR, Halpern D, Filoche M, Sapoval B, Grotberg JB. An asymptotic model of particle deposition at an airway bifurcation. Math Med Biol. 2013;30:131–56.
39. Choi S, Choi J, Lin CL. Contributions of Kinetic Energy and Viscous Dissipation to Airway Resistance in Pulmonary Inspiratory and Expiratory airflows in Successive symmetric airway models with various bifurcation angles. J Biomech Eng. 2018;140:0110101–01101013.
40. Oguma T, Hirai T, Niimi A, Matsumoto H, Muro S, Shigematsu M, Nishimura T, Kubo Y, Mishima M. Limitations of airway dimension measurement on images obtained using multi-detector row computed tomography. PLoS ONE. 2013;8:e76381.

Publisher's note